Kocatepe Veterinary Journal

Kocatepe Vet J. (2025):18(4):451-461

DOI: 10.30607/kvj.1639958

RESEARCH ARTICLE

Functional Anatomy of the Carpal Region in Sprague Dawley Strain Rats

Yasemin ÜSTÜNDAĞ[1*], Ümit KOÇAK[2], Belgin GIUOSEMOGLOU[2], Muhammed Ali AYDEMİR[3], Ahmet Berat YAKAR[2]

[1]Department of Anatomy, Faculty of Veterinary Medicine, Dokuz Eylul University, İzmir, Turkey
[2]Undergraduate Veterinary Student, Faculty of Veterinary Medicine, Dokuz Eylul University, İzmir, Turkey
[3]Undergraduate Veterinary Student, Faculty of Veterinary Medicine, Burdur Mehmet Akif Ersoy University, Burdur, Turkey

ABSTRACT

Dating back to 1830, Rattus norvegicus holds the distinction of being one of the first mammals domesticated for use in scientific researches. While detailed anatomical information about the human carpal region is available, such information is lacking for rats. The current study aims to resolve the ambiguity in the literature by determining which bones constitute the carpal bones of Sprague Dawley starin rats, the number and arrangement of these bones. Additionally, the study seeks to elucidate how the carpal tunnel, which is important in translational anatomy, is formed and which structures pass through it. In the study, seven 9-month-old female Sprague Dawley strain rats carpal regions were examined, macroscobically, morphometrically,and radiologically. The carpal bones of Sprague Dawley rats were examined and found to be arranged in two rows: proximal and distal A total of six carpal bones were identified, two in the proximal row and four in the distal row. The formation of the carpal tunnel in rats has been observed as follows. It is noted to form between the distal end of the antebrachium and the distal carpal bones. Compared to human and rat carpal bones and carpal tunnel, both of the structures are quite different each other. Therefore, it has been concluded that these rats are unsuitable for experimental surgical models, especially those focusing on the carpal region.

Keywords: Carpal bones, carpal tunnel, rat, Sprague Dawley, translational anatomy

****

Sprague Dawley Soyu Ratlarda Carpal Bölgenin Fonksiyonel Anatomisi

ÖZ

1830 yılına kadar uzanan geçmişiyle Rattus norvegicus, bilimsel araştırmalarda kullanılmak üzere evcilleştirilen ilk memelilerden biri olma özelliğini taşımaktadır. İnsan el bileği (karpal) bölgesine ait ayrıntılı anatomik bilgiler mevcutken, sıçanlar için bu tür bilgiler yetersizdir. Mevcut çalışma, literatürdeki belirsizlikleri gidermeyi amaçlayarak Sprague Dawley soyu sıçanların karpal kemiklerini, bu kemiklerin sayısını ve dizilimini belirlemeyi hedeflemektedir. Ayrıca, translasyonel anatomi açısından önemli olan karpal tünelin nasıl oluştuğunu ve hangi yapıların bu tünelden geçtiğini ortaya koymayı amaçlamaktadır. Çalışmada, 7 adet 9 aylık dişi Sprague Dawley soyu sıçanın karpal bölgesi makroskobik, morfometrik ve radyolojik yöntemlerle incelenmiştir. Sprague Dawley soyu sıçanların karpal kemiklerinin iki sıra halinde dizildiği gözlemlenmiştir: proksimal ve distal toplamda altı karpal kemik tespit edilmiş olup, bunların iki tanesi proksimal sırada, dört tanesi ise distal sırada yer almaktadır. Sıçanlarda karpal tünelin oluşumu şu şekilde gözlemlenmiştir: Antebrachium'un distal ucu ile distal karpal kemikler arasında bir tünel oluşmaktadır. İnsanlardaki ve sıçanlardaki karpal kemikler ve karpal tünel kıyaslandığında, bu yapıların birbirinden oldukça farklı olduğu belirlenmiştir. Bu nedenle, Sprague Dawley soyu sıçanların, özellikle karpal bölgeye odaklanan deneysel cerrahi modeller için uygun olmadığı sonucuna varılmıştır..

Anahtar Kelimeler: Karpal kemikler, karpal tünel, sıçan, sprague dawley, translasyonel anatomi

To cite this article: Üstündağ Y, Koçak Ü, Guosemoglu B, Aydemir MA, Yakar AB, Functional Anatomy of the Carpal Region in Sprague Dawley Strain Rats Kocatepe Vet J. (2025) 18(4) 451-461

Submission: 14.02.2025 **Accepted**: 03.12.2025 **Published Online**: 14.12.2025

ORCID ID; YÜ: 0000-0002-8836-0371; ÜK: 0009-0008-1281-8623; BG: 0009-0006-7314-1180; MAY: 0009-0005-4497-3650; ABY: 0009-0001-9336-6735
*Corresponding author e-mail: yasemin.ustundag@deu.edu.tr

INTRODUCTION

Operations addressing orthopaedic conditions that adversely affect people's quality of life often rely on animal models to predict success rates. The suitability of methods or materials tested in animal models can form the basis for transitioning to human applications. Dating back to 1830, Rattus norvegicus holds the distinction of being one of the first mammals domesticated for use in scientific researches (Iannaccone and Jacob 2009; Koolhaas 2010; Weber et al. 2019; Hashway and Smith 2020). Over time, rats stand out as the most commonly chosen animal model for biomedical purposes (Iannaccone and Jacob 2009). This is because rats are known to be genetically similar to humans (Babu et al. 2024). Rats also resemble humans in many ways, including their complex behaviours and physiological characteristics (Sharp and Villano 2012), and are frequently preferred in trauma models (Weber et al. 2019).

The carpal region in humans is a critical anatomical and functional area. It consists of the carpal bones, the median nerve, the flexor tendons of the fingers, and blood vessels. The median nerve is essential for hand dexterity and fine motor control, as it provides both sensory and motor functions to the thumb and the first three fingers (Asfar et al. 2023). With the advancement of technology, the increased use of computers, smartphones, and other digital devices has led to repetitive flexion and extension movements, as well as static loading in the wrist. Prolonged use of keyboards and mice, especially when combined with poor ergonomic practices, can elevate pressure within the carpal tunnel and cause thickening of the subsynovial connective tissue. This results in compression of the median nerve, leading to symptoms such as pain, numbness, and muscle weakness, which are characteristic of carpal tunnel syndrome (Dale et al. 2013; Padua et al 2023)

In recent years, many experimental studies have been carried out to investigate carpal tunnel syndrome (Collin et al. 2021; Çınar et al. 2024; Soito et al. 2024; Kroiwa et al. 2025; Zhou et al. 2025) . However, the comparative anatomy of rats and humans is not fully understood. While detailed anatomical information about the human carpal region is available, such information is lacking for rats. In particular, there are varying descriptions regarding the number and arrangement of carpal bones, and detailed information about the formation of the carpal tunnel is scarce. The current study aims to resolve the ambiguity in the literature by determining which bones constitute the carpal bones of Sprague Dawley starin rats, the number and arrangement of these bones. Additionally, the study seeks to elucidate how the carpal tunnel, which is important in translational anatomy, is formed and which structures pass through it. Because comprehensive literature reviews indicate that studies on the carpal region most commonly prefer rabbits (Ettema et al 2006; Tung et al. 2010; Çınar et al. 2024; Kroiwa et al. 2025; Zhou et al. 2025), followed by rats (Ettema et al. 2006; Tung et al. 2010; Collin et al. 2021; Soito et al. 2024) . Additionally, the suitability of dogs (Turan and Bolukbasi 2004; Ettema et al. 2006; Tung et al. 2019) , baboons (Ettema et al. 2006), and previously, primates (Mackinnon et al. 1985), has also been assessed.

MATERIALS and METHODS

In the study, seven 9-month-old female Sprague Dawley strain rats weighing between 750 and 850 grams were used. The rats cadavers included in the study were obtained from rat cadavers used in various projects conducted at the Dokuz Eylül University Multidisciplinary Experimental Animal Laboratory. Dokuz Eylül University Local Ethics Committee for Animal Experiments granted the ethics committee approval for the study with reference number 14/2024, dated 17.04.2024.

The carpal region was inspected macroscopically under the iPhone15 Pro Max (Apple Inc., Cupertino, CA, ABD) digital camera with 3x magnification. The location of the carpal bones and the transverse carpal ligament, the formation of the carpal tunnel, and the arrangement of the tendons and nerves passing through this tunnel have been determined by traditional dissection methods.

Following the traditional dissection procedure, radiographs of the carpal region were taken in the dorsoplantar and planto-dorsal directions using an X-ray device with a power of 0.5 kW, an exposure range of 0-32315 mAs, an exposure time of 0.01–6.3 seconds, and an operating frequency of 30 kHz, utilising the high inverter method with PWM. The x-ray images were recorded in Dicom format. The length and width of the bones in the X-ray images, , were measured using the Radiant software (Medixant, Poznań, Poland).

Then, organic tissues were removed from the skeletons, which were macerated by boiling for 30 minutes. After the maceration process, the tissue remaining on the skeletons was carefully cleaned. The bones in the region were separated from each other. Morphometric measurements of each animal's carpal bones, including the length, width, and breadth of each bone, were taken using a calibrated electronic digital calliper.

Statistics

All morphometric and digital data were subjected to a homogeneity test of variances. An Independent Samples T-Test was applied to observe whether there were any statistically significant differences between the data obtained from the right and left sides using both methods, as well as between the methods themselves. Statistically significant differences were considered at $p < 0.05$ level. All results were presented

as maximum, minimum, mean, and standard deviation (Table 1,2 and 3). All statistical analyses were performed using IBM SPSS version 29 (Chicago, USA).

Table 1. Descriptive statistics of measurements of the right and left carpal bones by digital caliper

Width of OCIV	**7**	**0.54**	**0.75**	**0.6414**	**0.06492**	**Width of OCIV**	**7**	**0.55**	**1.46**	**0.8243**	**0.31464**
Right	**N**	**Minimum**	**Maximum**	**Mean**	**Std. Deviation**	**Left**	**N**	**Minimum**	**Maximum**	**Mean**	**Std. Deviation**
Length of OCU	7	1.57	3.16	2.7057	0.52399	**Length of OCU**	7	2.38	2.91	2.7557	0.18618
Heigth of OCU	7	1.21	1.91	1.6157	0.25922	**Heigth of OCU**	7	1.35	2.13	1.7900	0.26552
Width of OCU	7	0.75	1.32	1.1357	0.20550	**Width of OCU**	7	0.91	1.40	1.1029	0.15924
Length of OCR	7	1.87	2.30	2.0286	0.14369	**Length of OCR**	7	1.57	2.16	1.8929	0.19233
Heigth of OCR	7	1.17	1.59	1.4629	0.16327	**Heigth of OCR**	7	1.30	1.86	1.6471	0.19224
Width of OCR	7	0.77	1.01	0.9057	0.08561	**Width of OCR**	7	0.75	1.01	0.8657	0.08886
Length of OCI	7	2.25	3.54	2.8543	0.44855	**Length of OCI**	7	2.67	4.05	3.3457	0.53740
Heigth of OCI	7	1.08	1.75	1.2886	0.22282	**Heigth of OCI**	7	1.17	1.60	1.3243	0.16910
Width of OCI	7	0.56	1.02	0.8014	0.15302	**Width of OCI**	7	0.44	0.97	0.6843	0.16267
Length of OCII	7	1.73	2.69	2.0857	0.37443	**Length of OCII**	7	1.74	2.47	2.0386	0.29785
Heigth of OCII	7	1.03	1.69	1.3357	0.24832	**Heigth of OCII**	7	1.01	1.63	1.4700	0.22226
Width of OCII	7	0.61	0.92	0.7643	0.09641	**Width of OCII**	7	0.66	0.98	0.7700	0.11590
Length of OCIII	7	1.66	2.53	2.1271	0.31627	**Length of OCIII**	7	1.06	2.63	1.7829	0.56785
Heigth of OCIII	7	1.24	1.69	1.4871	0.14488	**Heigth of OCIII**	7	0.95	1.59	1.2857	0.22759
Width of OCIII	7	0,60	1.08	0.8529[a]	0.15713	**Width of OCIII**	7	0.52	0.89	0.6629[b]	0.13475
Length of OCIV	7	2.35	4.03	3.3271	0.56177	**Length of OCIV**	7	2.06	3.18	2.7543	0.38492
Heigth of OCIV	7	1.01	1.60	1.3143	0.17672	**Heigth of OCIV**	7	0.84	1.57	1.2086	0.29639

OCU: Os carpi ulnare, **OCR:** Os carpi radiale, **OCI:** Os carpale I, **OCII:** Os carpale II, **OCIII:** Os carpale III, **OCIV:** Os carpale IV

Table 2. Descriptive statistics of measurements of the right and left carpal bones from radiographic images

Right	N	Minimum	Maximum	Mean	Std. Deviation	Left	N	Minimum	Maximum	Mean	Std. Deviation
Length of OCU	7	1.79	3.34	2.7643	0.47888	**Length of OCU**	7	2.57	3.03	2.8271	0.13647
Heigth of OCU	7	1.49	1.87	1.7371	0.14080	**Heigth of OCU**	7	1.51	2.27	1.8229	0.25025
Length of OCR	7	1.64	2.18	1.9229	0.18563	**Length of OCR**	7	1.73	2.42	2.0000	0.24331
Heigth of OCR	7	1.34	1.68	1.5200	0.12897	**Heigth of OCR**	7	1.38	2.18	1.7271	0.26399
Length of OCI	7	2.21	4.77	3.0143	0.83076	**Length of OCI**	7	2.61	3.86	3.3443	0.49789
Heigth of OCI	7	1.11	1.80	1.3643	0.22744	**Heigth of OCI**	7	1.27	1.60	1.4406	0.14661
Length of OCII	7	1.60	2.84	2.0529	0.46425	**Length of OCII**	7	1.79	2.38	2.0314	0.25056
Heigth of OCII	7	1.17	1.64	1.3986	0.16324[a]	**Heigth of OCII**	7	1.41	1.63	1.5686[b]	0.08783
Length of OCIII	7	1.78	3.05	2.3757	0.41577	**Length of OCIII**	7	1.04	2.63	1.8886	0.57514
Heigth of OCIII	7	1.28	1.92	1.6171	0.24951[a]	**Heigth of OCIII**	7	0.85	1.64	1.2800[b]	0.29743
Length of OCIV	7	3.34	4.60	3.8986	0.43122[a]	**Length of OCIV**	7	2.17	3.44	2.8329[b]	0.43188
Heigth of OCIV	7	1.16	1.87	1.5243	0.25631	**Heigth of OCIV**	7	0.86	1.80	1.3371	0.34389

OCU: Os carpi ulnare, **OCR:** Os carpi radiale, **OCI:** Os carpale I, **OCII:** Os carpale II, **OCIII:** Os carpale III, **OCIV:** Os carpale IV

Table 3. Descriptive statistics of measurements of the retinaculums by digital caliper

		N	Mean	Std. Deviation
Heigth of TRC	**Right**	7	5.4886	0.08194
	Left	7	5.5043	0.10081
Length of TRC	**Right**	7	4.1829	0.16919
	Left	7	4.2229	0.18145

TRC: Transverse Carpal Ligament

RESULTS

Morphology

The carpal bones of Sprague Dawley rats were examined and found to be arranged in two rows: proximal and distal. A total of six carpal bones were identified, two in the proximal row and four in the distal row. The proximal row consists of the os carpi radiale and os carpi ulnare, while the distal row is composed of the os carpale I, II, III, and IV (Figure 1).

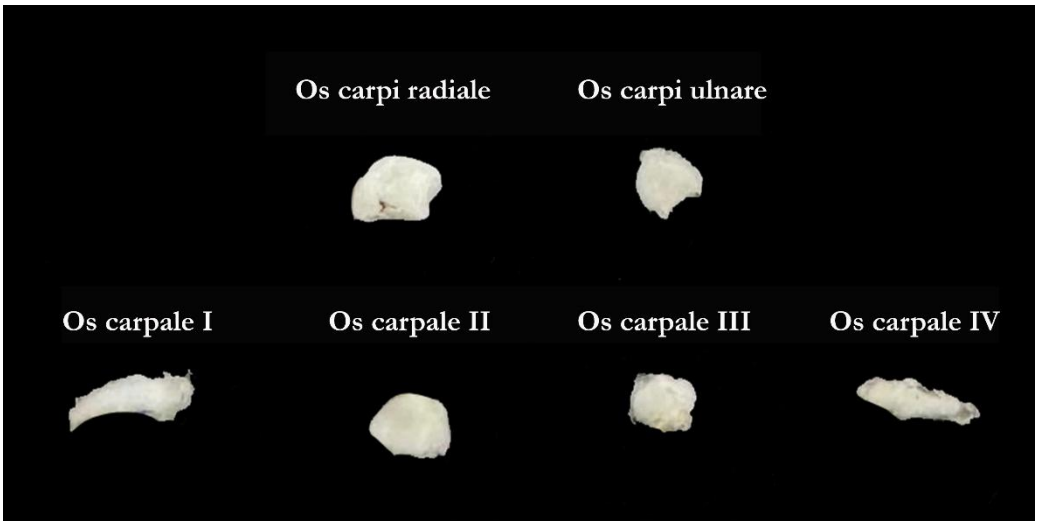

Figure 1: Definition of carpal bones in proximal and distal row

In terms of morphology, the os carpi radiale resembles the shape of a quarter-circle. The os carpi ulnare and os carpale II exhibit a rectangular-like shape, while the os carpale III has a cuboid structure. The os carpale I and os carpale IV are thin and hook-shaped, curving towards the central region of the carpal area. Their free ends face each other, with an almost negligible gap or a maximum separation of approximately 0.1 mm between them.

When examined in terms of their articulations, the os carpi radiale articulates proximally with the distal end of the radius and distally with os carpale I and os carpale II. The os carpi ulnare articulates proximally with the distal end of the ulna and distally with os carpale III and os carpale IV. The os carpale I articulates laterally with os carpale II and distally with os metacarpale I. The os carpale II articulates distally with os metacarpale I, II, and III, and laterally with os carpale I and os carpale II. The os carpale III articulates distally with os metacarpale IV and V, and laterally with os carpale II and os carpale IV. The os carpale IV articulates distally with os metacarpale V and laterally with os carpale III (Figure 2, 3 and 4).

,

Figure 2: Dorsal view of carpal bones and their boundaries **1:** Os carpi radiale, **2:** Os carpi ulnare, **3:** Os carpale II, **4:** Os carpale III

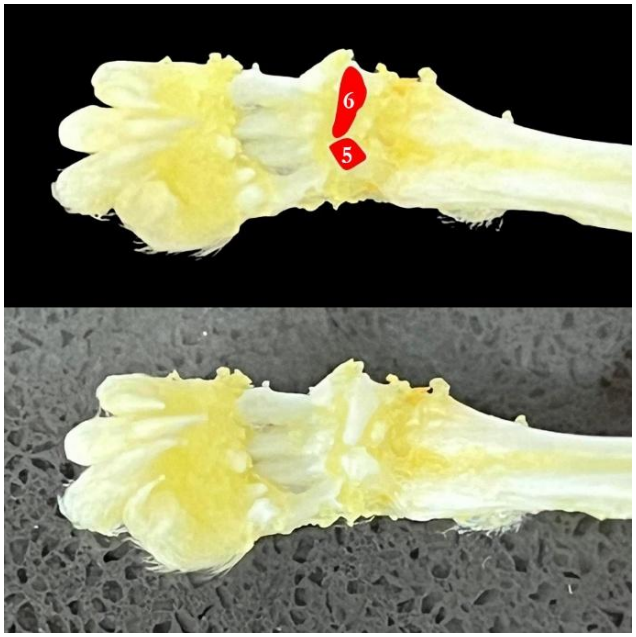

Figure 3: Palmar view of carpal bones and their boundaries **5:** Os carpale I, **6:** Os carpale IV

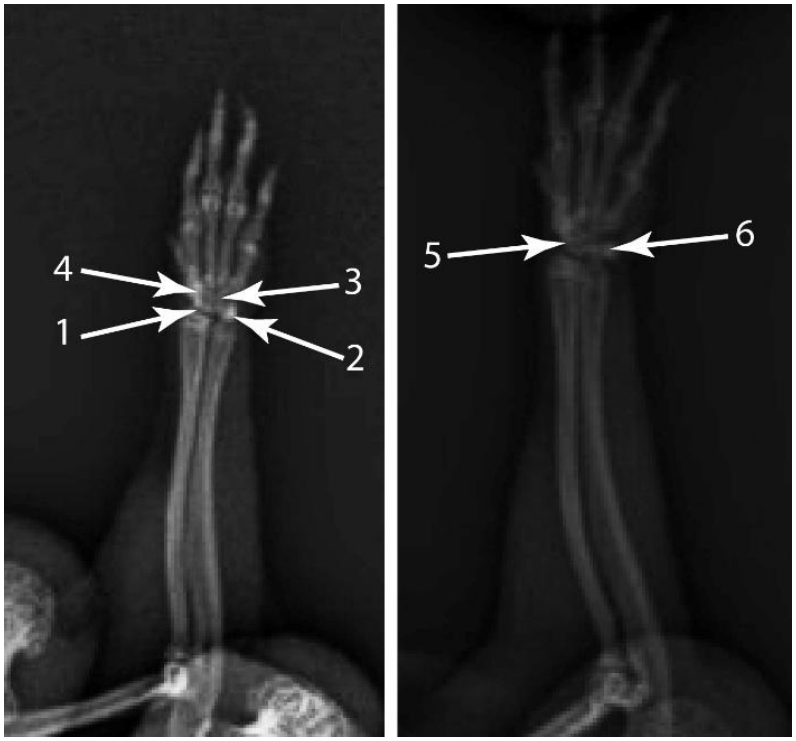

Figure 4: Radiographic images of carpal bones **1:** Os carpi radiale, **2:** Os carpi ulnare, **3:** Os carpale II, **4:** Os carpale III, **5:** Os carpale I, **6:** Os carpale IV

The formation of the carpal tunnel in rats has been observed as follows. It is noted to form between the distal end of the antebrachium and the distal carpal bones. The transverse carpal ligament begins approximately 2,44 mm from the distal end of the antebrachium and terminates at the end of the distal row of carpal bones (Figure 5). On the right side, it extends between the distal end of the radius and os carpale I, while on the left side, it spans between the distal end of the ulna and os carpale IV (Figure 6). In terms of its attachment, it appears to have a loose structure.

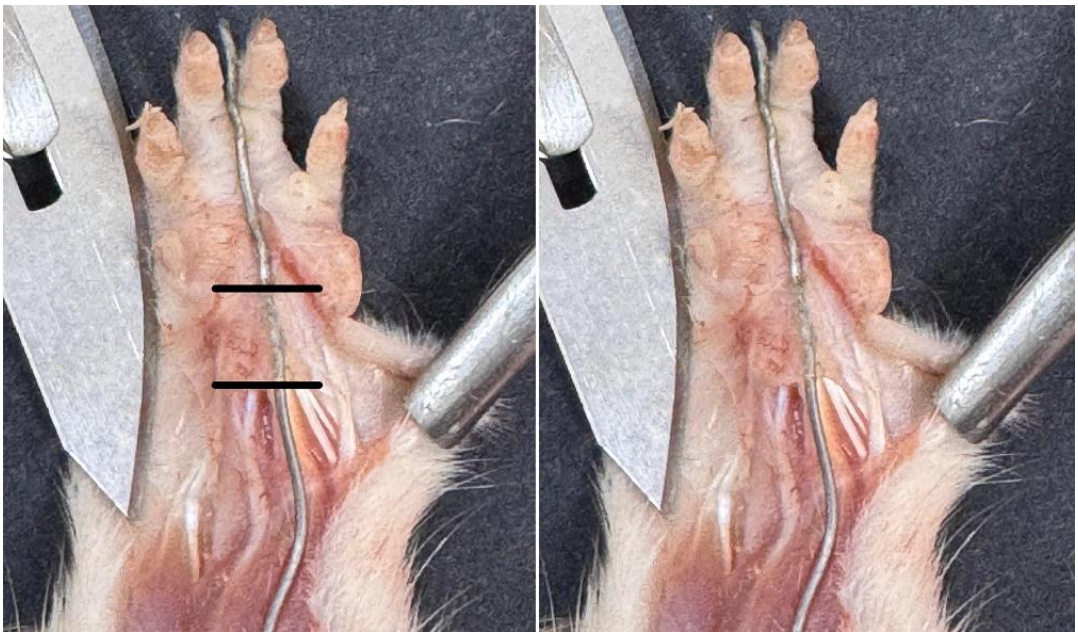

Figure 5. Proximal and distal boundaries of transverse carpal ligament

Figure 6. View of os carpale II and IV after transranverse carpal ligament removal

The structures passing through the tunnel include three tendons of the musculus (m). flexor digitorum superficialis, three tendons of the m. flexor digitorum profundus, the tendon of the m. palmaris longus, and the nervus (n.) medianus. Their arrangement within the tunnel is as follows: superficially, the tendon of the m. palmaris longus is located most medially, and adjacent to it lies the n. medianus, and finally, the tendons of the m. flexor digitorum superficialis. Profoundly, the tendons of the m. flexor digitorum profundus are situated (Figure 7).

Figure 7. Structures passing through transranverse carpal ligament superficially and surrounding muscles**a:** M. flexor carpi ulnaris, **b:** M. flexor digitorum superficialis, **c:** N.medianus, **d**: M. palmaris longus, **e:** M.flexor carpi radilais, **f:** M. extensor carpi longus, **g:** M. brachialis M.flexor digitorum superficialis, n medianus and m. palmaris longus pass through the transverse carpal ligament.

Statistics

According to the Independent Samples t-test results for data obtained using a digital calliper for the right and left sides, a significant difference was observed only in the width of os carpale III ($p<0.05$). Based on the Independent Samples t-test results for data obtained from radiographic images of the right and left sides, a significant difference was found in the height of os carpale II, the height of os carpale III ($p<0.05$), and the length of os carpale IV ($p<0.001$). No statistically significant difference was found between the data obtained from the digital calliper and radiographic images or between the data of the right and left transverse carpal ligament.

DISCUSSION

Detailed literature reviews have revealed a notable ambiguity about carpal bones in rats. Although various statements regarding the number and arrangement of these bones exist, no detailed information pertaining to their morphology has been documented.

Hunt (1924) defined the number of carpal bones as "There are nine carpal bones." According to Chiasson (1994), the carpal bones are arranged in two rows of bones: proximal and distal. However, between these two rows lies an os carpi centrale. The proximal row is formed by the os carpi radiale and os carpi ulnare, while os carpale I-IV forms the distal row. The os pisiforme is a small bone that provides lateral support to the wrist. Smith and Schenk (2001) & Tung et al. (2010) reported that rats have two rows of carpal bones. In the proximal row, they identified the os pisiforme, os triangulare, os lunatum, and os naviculare, while the distal row consists of the os hamatum, os capitatum, and os falciforme. In summary, it has been stated that the proximal row comprises four bones, and the distal row consists of three bones (Tung et al. 2010). Maynard and Downes (2019) stated that the skeletal structure of the carpal region consists of carpal bones, which extend between the radius and ulna and the metacarpal bones. They further noted that, even in large mammals such as humans, the carpal bones are relatively small, while in rats, they are present as small nodules. According to Maynard and Downes (2019), the carpal bones are arranged in three rows: proximal, middle, and distal. They identify the proximal row as consisting of three bones: the os carpi intermedio-radiale, os carpi ulnare, and os pisiforme. The middle row comprises a single bone, the os carpi centrale, while the distal row consists of four bones: the os trapezium, os trapezoideum, os capitatum, and os hamatum.

As demonstrated in the given examples, the inconsistency in the literature is expected to cause further confusion in future modelling efforts. Addressing this discrepancy in the literature is the primary objective of this study. The present study's findings do not align with the existing literature (Hunt 1924; Chiasson 1994; Tung et al. 2010; Maynard and Downes 2019). In this study, the carpal bones were observed to be arranged in two rows: proximal and distal, with two bones in the proximal row and four bones in the distal row. The nomenclature was determined based on their anatomical location in accordance with the Nomina Anatomica Veterinaria (WAVA, 2017). However, compared to human carpal bones, they differ in terms of arrangement, number, and morphology (White et al. 2012; Hajizadeh et al. 2021).

Maynard and Downes (2019) highlighted the importance of identifying the counterparts of rat carpal bones in humans for anatomical education from a translational perspective. This is particularly significant as the wrist joints of certain rat strains, such as Wistar Albino (Xia et al. 2018) and Lewis (Lim et al. 2017), have been shown to be crucial in modelling diseases related to arthritis and repetitive wrist injuries (Driban et al. 2011; Xia et al. 2018; Hajizadeh et al. 2021). According to the present study's findings, the carpal region in Sprague Dawley rats was relatively small. However, if this strain has a genetic predisposition to experimentally induced arthritis, it may be considered a potential alternative to the Wistar Albino and Lewis strains.

Another aim of the the present study it to evaluate bilateral morphological differences in the carpal region using both direct measurements obtained with a digital calliper and radiographic analysis. The Independent Samples t-test revealed that significant asymmetry between the right and left sides was limited to the width of os carpale III when using digital calliper measurements ($p < 0.05$). This suggests a potential unilateral variation in carpal morphology, which could be influenced by hand dominance or functional loading patterns or malnutrition in growth, as reported in previous studies on skeletal asymmetry (Sharma et al., 2014). Radiographic assessment, however, demonstrated a broader range of significant differences, including the height of os carpale II and III ($p < 0.05$) and the length of os carpale IV ($p < 0.001$). These findings may indicate that imaging-based evaluation provides enhanced sensitivity in detecting dimensional variations that are not easily captured through direct measurements. Such differences could be attributed to subtle positional or structural adaptations, highlighting the value of radiographic analysis for detailed morphometric studies.

One of the conditions that may be encountered in the wrist region is carpal tunnel syndrome. Carpal tunnel syndrome is a common hand disorder characterised by the median nerve compression at the wrist. Although most cases are described as idiopathic, repetitive hand use has been identified as a contributing factor in some instances (Tung et al. 2010). Following the recognition that the pathophysiology of carpal tunnel syndrome is related to the compression of the median nerve at the carpal tunnel level, surgical interventions have been developed to alleviate this compression. The primary goal of surgical treatment is to increase the volume of the carpal tunnel by releasing the transverse carpal ligament (Dunken and Kakinoki 2017; Orhurhu et al. 2020; Pripotnev and Mackinnon 2022; Moeller et al. 2024). Ongoing research continues to explore new approaches for treating carpal tunnel syndrome. However, directly applying new procedures to human subjects may pose ethical and safety concerns. Consequently, there is an increasing need for experimental studies in the biomedical field. For this purpose, female rats were preferred as the experimental model in the current study since carpal tunnel syndrome is more prevalent among women and older individuals (Dale et al. 2013; Newington et al. 2015; Wright and Atkinson 2019; Osiak et al. 2022).

In humans, the carpal tunnel is a narrow, inflexible passage on the wrist's palmar aspect. It is bounded anteriorly by the transverse carpal ligament, the central portion commonly termed the transverse carpal ligament. Posteriorly, the tunnel is defined by the concave volar surface of the carpal bones, forming the carpal sulcus. The lateral boundary of the carpal sulcus is demarcated by the radio-carpal eminence, comprising the tubercles of the scaphoid and trapezium bones, while the medial border is formed by the tubercles of the pisiform and the hook of the hamate, collectively referred to as the ulnar carpal eminence (White et al. 2012; Osiak et al. 2022; Kaiser et al. 2024). The proximal extent of the carpal tunnel originates at the volar wrist crease. It extends distally, spanning from the lateral border of the abducted thumb to the level of the hamate's hook. Within this tunnel, the median nerve and nine flexor tendons are housed. These tendons include one for the flexor pollicis longus, four for the flexor digitorum superficialis, and four for the flexor digitorum profundus. The median nerve, positioned most superficially, lies atop the flexor digitorum superficialis and flexor digitorum profundus tendons associated with the index finger. The nerve traverses the carpal tunnel, passing beneath the transverse carpal ligament to enter the volar region of the hand (White et al. 2012; Osiak et al. 2022; Kaiser et al. 2024).

In Sprague Dawley strain rats, the formation of the carpal tunnel, the structure of the transverse carpal ligament, and the structures passing through the ligament are completely different from those in humans. The transverse carpal ligament is wider and has a looser structure than in humans. The ligament, unlike in humans, extends from the distal end of the radius and ulna to the lower border of the distal row of carpal bones. The current study's findings support González-Rellán et al.'s (2023) study. In that study, González-Rellán et al. (2023) showed that the transverse carpal ligament extended between the antebrachiocarpal and the carpometacarpal joints. That means, the wrists and their internal structures demand greater protection in quadrupedal mammals. Although rats display some bipedal characteristics, they remain primarily quadrupedal, and the broad transverse carpal ligament provides enhanced stabilisation of the carpal tunnel.

In addition, the tunnel is supported not only by this ligament but also by the carpal bones, which are arranged in a ring-like formation. The carpal tunnel accommodates several structures, including both three tendons of the flexor digitorum superficialis and the flexor digitorum profundus, the palmaris longus tendon, and the median nerve. These structures are arranged in the following manner: superficially, the palmaris longus tendon is found on the medial side,

next to which lies the median nerve and then the tendons of the flexor digitorum superficialis. The first and fourth carpal bones are positioned in a circular, ring-like manner over these structures. Deeper within the tunnel, the flexor digitorum profundus tendons are positioned.

The palmaris longus muscle is a rare and weak flexor muscle of the wrist found in only a small human population. It has been suggested that the palmaris longus tendon could serve as a distinct risk factor associated with carpal tunnel syndrome (Duncan and Kakinoki 2017). According to the current study's findings, the presence of the palmaris longus tendon might suggest the potential for median nerve compression. However, in contrast, it is hypothesised that in Sprague Dawley strain rats, this tendon is unlikely to contribute to carpal tunnel syndrome due to the loose structure of the transverse carpal ligament and the protective, ring-like arrangement of the carpal bones, which safeguard the structures within this region.

Research on the formation of the carpal tunnel in various animal species is well-documented in the literature. One notable study is by Ettema et al. (2006), highlighted the comparative anatomical study of the sub-synovial connective tissue in the carpal tunnel of rats, rabbits, dogs, baboons, and humans. Additionally, Turker Yavas et al. (2024), along with Turker Yavas and Dabanoglu (2024), eluciated the structure of the carpal tunnel in rabbits. In Ettema et al.'s study, anatomical details of the carpal region in rats were not provided, and it was only mentioned that the tunnel is narrow. The current study's findings support Ettema et al.'s, study. Also, Turker Yavas et al. and Turker Yavas and Dabanoglu validated that rabbits may be suitable anatomically for carpal tunnel syndrome research. Based on these findings of existing literature, current study demonstrated that Sprague-Dawley strain rats do not serve as a good model for investigating the neuropathological changes induced by median nerve compression in the carpal tunnel and Sprague Dawley strain rats should not be preferred for experimental carpal tunnel syndrome research.

CONCLUSION

The results of this study, when compared with the literature, reveal that the anatomy of the carpal region in Sprague Dawley rats does not resemble that of humans, particularly concerning carpal tunnel morphology. Therefore, it has been concluded that these rats are unsuitable for experimental surgical models, especially those focusing on the carpal region. On the other hand, the limitation of the current study is that it was conducted on only a single strain of rats. Further research into the anatomy of the carpal region in other frequently used rat strains as laboratory animals, is suggested.

Conflict of interest: The authors have no conflicts of interest to report.

Authors' Contributions: YÜ and ÜK contributed to the project idea, design and execution of the study. ÜK, BG, ABY and MAA contributed to the acquisition of data. YÜ analysed the data. YÜ, ÜK, BG, ABY and MAA drafted and wrote the manuscript. YÜ reviewed the manuscript critically. All authors have read and approved the finalized manuscript.

Ethical approval: This study was carried out at Dokuz Eylül University Faculty of Veterinary Medicine. This research was approved by The Dokuz Eylül University Local Ethics Committee for Animal Experiments(Ref No: 14/2024, Date: 02.08.2024)

Acknowledgement : This study was supported by TÜBİTAK with 2209-A -Research Project Support Programme for Undergraduate Students (2023/2), Project Number: 1919B012320373

REFERENCES

Babu, H. A., Sai, A. R., Bandavi, B. K., Jyothsna, M., Snehitha, B., Reddy. K. S. & Pasala, P. K. (2024). An Updated Review on Rat Genetics and Genomics: Understanding Complex Traits and Diseases. Uttar Pradesh Journal of Zoology, 45(9), 74-75.

Chiasson, R. B. (1994). Laboratory of the White Rat. Fifth Edition. WCB/McGraw-Hill.

Collin, A., Vein, J., Wittrant, Y., Pereira, B., Amode, R., Guillet, C., Richard, D., Eschalier, A., & Balayssac, D. (2021). A new clinically-relevant rat model of letrozole-induced chronic nociceptive disorders. Toxicology and Applied Pharmacology, 425, 115600. https://doi.org/10.1016/j.taap.2021.115600

Çınar, S., Turan, E., & Akkoç, A. N. (2025). Establishing the electrophysiological feasibility of the rabbit median nerve as an experimental model for carpal tunnel syndrome. Journal of Neuroscience Methods, 418, 110411. https://doi.org/10.1016/j.jneumeth.2025.110411

Dale, A. M., Harris-Adamson, C., Rempel, D., Gerr, F., Hegmann, K., Silverstein, B., Burt, S., Garg, A., Kapellusch, J., Merlino, L., Thiese, M. S., Eisen, E. A., & Evanoff, B. (2013). Prevalence and incidence of carpal tunnel syndrome in US working populations: pooled analysis of six prospective studies. Scandinavian Journal of Work, Environment & Health, 39(5), 495-505. doi: 10.5271/sjweh.3351.

Driban, J. B., Barr, A. E., Amin, M., Sitler, M. R.,& Barbe, M. F. (2011). Joint inflammation and early degeneration induced by high-force reaching are attenuated by ibuprofen in an animal model of work-related musculoskeletal disorder. Journal of Biomedicine and Biotechnology, 2011, 691412. doi: 10.1155/2011/691412.

Duncan, S. F. M., & Kakinoki, R. (2017). Carpal Tunnel Syndrome and Related Median Neuropathies.Springer International Publishing AG . DOI 10.1007/978-3-319-57010-5

Ettema, A. M., Zhao, C., An, K.N., & Amadio, P.C. (2006). Comparative anatomy of the subsynovial connective tissue in the carpal tunnel of the rat, rabbit, dog, baboon, and human. Hand, 1(2), 78-84. doi: 10.1007/s11552-006-9009-z.

González-Rellán, S., Fdz-de-Trocóniz, P., & Barreiro A. (2023). Ultrasonographic anatomy of the palmar region of the carpus of the dog. Veterinary Radiology & Ultrasound, 64(3), 546-556. doi: 10.1111/vru.13224.

Hajizadeh, A., Abtahi Froushani, S. M., Tehrani, A. A., Azizi, S., & Bani Hashemi, S. R. (2021). Effects of Naringenin on Experimentally Induced Rheumatoid Arthritis in Wistar Rats. Archives of Razi Institute, 76(4), 903-912. doi: 10.22092/ari.2020.351612.1527.

Hashway, S. A., & Wilding, L. A. (2020). Translational Potential of Rats in Research. The Laboratory Rat. Academic Press. doi:10.1016/b978-0-12-814338-4.00003-9

Hunt, H. R. (1924). The laboratory manual of the anatomy of the rat. The MacMillan Company.

Iannaccone, P., & Jacob, H.J. (2009). Rats!. Disease Models & Mechanisms, 2, 206-210. doi:10.1242/dmm.002733

Kaiser, P., Schmidle, G., Bode, S., Seeher, U., Honis, H. R., Moriggl, B., Pechriggl, E., Stofferin, H., & Konschake, M. (2024) Clinical-applied anatomy of the carpal tunnel regarding mini-invasive carpal tunnel release. Archives of Orthopaedic and Trauma Surgery, 144(11), 4753-4765. doi: 10.1007/s00402-024-05560-7.

Koolhaas, J.M. (2010). The UFAW handbook on the care and management of laboratory and other research animals. 8th ed. John Wiley and Sons.

Kuroiwa, T., Lui, H., Nakagawa, K., Iida, N., Desrochers, C., Wan, R., Nishimura, K., Adam, E., Larson, D., Amadio, P., & Gingery, A. (2025, May 13). Influence of high-fat diet and sex on connective tissue in carpal tunnel syndrome. bioRxiv. https://doi.org/10.1101/2023.07.15.549152

Lim, M. A., Louie, B., Ford, D., Heath, K., Cha, P., Betts-Lacroix, J., Lum, P. Y., Robertson, T. L., & Schaevitz, L. (2017). Development of the Digital Arthritis Index, a Novel Metric to Measure Disease Parameters in a Rat Model of Rheumatoid Arthritis.
Frontiers in Pharmacology, 8, 818. doi: 10.3389/fphar.2017.00818.

Mackinnon, S. E., Dellon, A. L., Hudson, A. R., & Hunter, D. A. (1985). A primate model for chronic nerve compression. Journal of Reconstructive Microsurgery, 1(3), 185–195. https://doi.org/10.1055/s-2007-1007073

Maynard, R. L., & Downes, N. (2019). Anatomy and Histology of the Laboratory Rat in Toxicology and Biomedical Research. Elsevier Academic Press.

Moeller, E., Krasnoff, C. C., Hathaway, B. A., Kamenko, S., Burch, S., Carboy, J., & Solomon, J. S. (2024). Predicting thenar motor branch anatomy for a safer carpal tunnel release. Clinical Neurology and Neurosurgery, 246, 108606. doi: 10.1016/j.clineuro.2024.108606.

Newington, L., Harris, E. C., & Walker-Bone, K. (2015). Carpal tunnel syndrome and work. Best Practice & Research Clinical Rheumatology, 29(3), 440-453. doi: 10.1016/j.berh.2015.04.026.

Orhurhu, V., Orman, S., Peck, J., Urits, I., Orhurhu, M. S., Jones, M. R., Manchikanti, L., Kaye, A. D., Odonkor, C., Hirji, S., Cornett, E. M., Imani, F., Varrassi, G., & Viswanath, O. (2020). Carpal Tunnel Release Surgery- A Systematic Review of Open and Endoscopic Approaches. Anesthesia and Pain Medicine, 10(6), e112291. doi: 10.5812/aapm.112291.

Osiak, K., Elnazir, P., Walocha, J. A., & Pasternak, A. (2022). Carpal tunnel syndrome: state-of-the-art review. Folia Morphologica, 81(4), 851-862. doi: 10.5603/FM.a2021.0121.

Pripotnev, S., &Mackinnon, S. E. (2022). Revision of Carpal Tunnel Surgery. Journal of Clinal Medicine, 11(5), 1386. doi: 10.3390/jcm11051386.

Saito, K., Okada, M., Yokoi, T., Hama, S., & Nakamura, H. (2024). Fluorescein angiography for monitoring neural blood flow in chronic nerve compression neuropathy: Experimental animal models and preliminary clinical observations. Neurology International, 16(5), 976–991. https://doi.org/10.3390/neurolint16050074

Sharp, P., & Villano, J. S. (2012). The laboratory rat. CRC press.

Sharma, S., Mishra, V., & Kulshreshtha, V. (2014). Radiographical study showing asymmetry in the surface area of carpal bones in malnourished children. Journal of Clinical and Diagnostic Research, 8(6), AC08–AC10. https://doi.org/10.7860/JCDR/2014/8993.4505

Smith, D. G., & Schenk, M .P. (2001). A dissection guide and atlas to the rat. Morton Publishing Company.

Tung , W. L., Zhao, C., Yoshii, Y., Su , F. C., An, K. N., & Amadio, P. C. (2010). Comparative study of carpal tunnel compliance in the human, dog, rabbit, and rat. Journal of Orthopaedic Research, 28(5), 652-656. doi: 10.1002/jor.21037.

Turan, E., & Bolukbaşı, O. (2004). Evaluation of possible carpal tunnel syndrome in dogs. Veterinary Record, 155(4), 122–124. https://doi.org/10.1136/vr.155.4.122

Turker Yavas, F., Dabanoglu, I., & Akkoc, A.N. (2024). Anatomical Structures in the Rabbit Carpal Tunnel: Comparison with Human. Slovenian Veterinary Research, 61, 3, 187. DOI 10.26873/SVR-1870-2023

Turker Yavas, F., & Dabanoglu, I. (2024). Morphological characteristics of rabbits' carpal tunnel: Evaluation of its potential for carpal tunnel research. Journal of the Hellenic Veterinary Medical Society, 75(3), 8073–8082. https://doi.org/10.12681/jhvms.37030

Weber, B., Lackner, I., Haffner-Luntzer, M., Palmer, A., Pressmar, J., Scharffetter-Kochanek, K., & Kalbitz, M. (2019). Modeling trauma in rats: similarities to humans and potential pitfalls to consider. Journal of Translational Medicine, 17(1), 305. doi:10.1186/s12967-019-2052

White, T. D., Black, M. T., & Folkens, P. A. (2012). Human Osteology. Elsevier Academic Press.

World Association of Veterinary Anatomists (WAVA). (2017). Nomina anatomica veterinaria (6th ed.). International Committee on Veterinary Gross Anatomical Nomenclature.

Wright, A.R.,and Atkinson, R.E.(2019). Carpal Tunnel Syndrome: An Update for the Primary Care Physician. Hawaii J Health Soc Welf, 78(11 Suppl 2),6-10.

Xia ZB, Yuan YJ, Zhang QH, Li H, Dai JL, & Min JK. (2018). Salvianolic Acid B Suppresses Inflammatory Mediator Levels by Downregulating NF-κB in a Rat Model of Rheumatoid Arthritis. Med Sci Monit, 24,2524-2532. doi: 10.12659/msm.907084.

Zhou, Q. Y., Li, T. H., Zeng, J. Y., Wu, D. T., Li, Y. N., Chen, Q., & Li, S. L. (2025). Comparison of the establishment of a rabbit model of carpal tunnel syndrome under ultrasound-guided and landmark-guided methods. Scientific Reports, 15(1), 8186. https://doi.org/10.1038/s41598-025-93429-z